Critical phases of antiferromagnetic Potts model on fractals

1986 J. Phys. A: Math. Gen. 19 3395

(http://iopscience.iop.org/0305-4470/19/16/034)

J. Phys. A: Math. Gen. 19 (1986) 3395-3406. Printed in Great Britain

Critical phases of antiferromagnetic Potts model on fractals

Rosane Riera

Department of Physics, Pontifícia Universidade Católica do Rio de Janeiro, 22453, Rio de Janeiro, Brazil

Received 20 August 1985, in final form 13 January 1986

Abstract. We study the q-state antiferromagnetic Potts model on fractals, namely the Sierpinski carpets ($1 < D_f < 2$) and pastry shells ($2 < D_f < 3$). For both families a critical value q_c was found, above which the system is always in the paramagnetic phase whereas for q at or less than q_c the system exhibits a low temperature critical phase. The phase diagrams are analysed from the geometrical point of view.

Recently, many investigators have concentrated on the influence of fractal geometries on the critical behaviour of ferromagnetic systems (Gefen *et al* 1984a, b, Riera 1985). An important new result that emerges from these studies is the relevance of other geometrical parameters, apart from the dimensionality, in defining universality classes. Since antiferromagnetic systems in Euclidean lattices have local geometrical properties influencing the critical behaviour, the study of these systems on fractal geometries is in order. In particular, it is interesting to study systems with non-zero ground state entropy per site, such as the antiferromagnetic Potts model, and investigate the existence of a critical value q_c above which there is only the paramagnetic phase. Also, as suggested for hypercubic lattices (Berker and Kadanoff 1980), one hopes that, for $q \leqslant q_c$, the low temperature phase may be characterised by an algebraic decay of correlations; thus for any $T \leqslant T_c$, the correlation length is infinite.

In this paper, we use an approximate renormalisation group (RG) approach for the antiferromagnetic (AF) Potts model on two types of self-similar fractals, namely the Sierpinski carpet and the Sierpinski pastry shell (Mandelbrot 1977), following a previous study of the ferromagnetic case on these lattices (Riera and Chaves 1986). In what follows, we briefly discuss the fractal geometries considered in this work and the general form of the RG equations. Results for the carpet and pastry families are then discussed with special attention to the phase diagrams obtained.

Figure 1 shows examples of self-similar fractal lattices called the Sierpinski carpet and Sierpinski pastry shell. The first (second) family is constructed by an iterated subdivision of a unit square (cube) into b^2 (b^3) small ones and the simultaneous cutout of l^2 (l^3) small ones. The fractal dimension (Mandelbrot 1977) is defined as

$$D_f = \ln(b^2 - l^2)/\ln b \tag{1a}$$

or

$$D_f = \ln(b^3 - l^3)/\ln b. \tag{1b}$$

The small squares (cubes) can be removed in two ways leading to geometries with different lacunarity L (Gefen *et al* 1984a) (different degree of homogeneity, see figure

0305-4470/86/163395+12$02.50

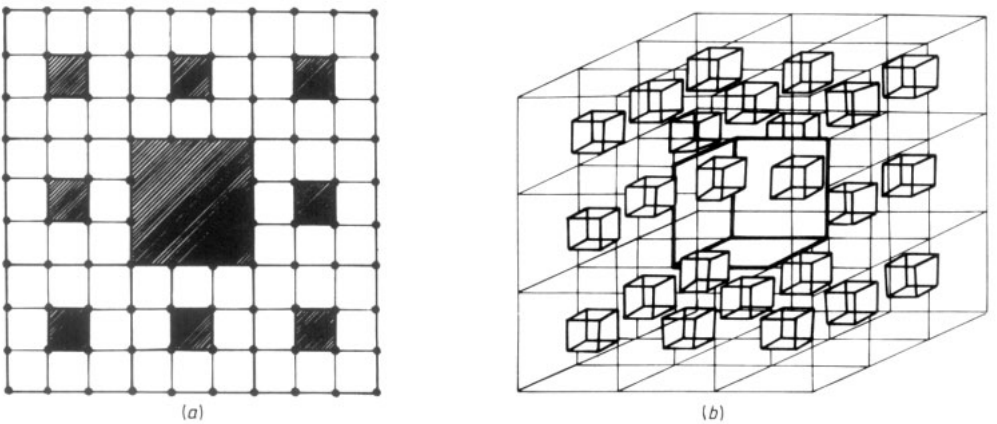

Figure 1. Sierpinski carpet (a) and Sierpinski pastry shell (b) with $b=3$, $l=1$ after two steps in the lattice construction. The lattice sites in (a) are denoted by ●; the location of sites in (b) follows a similar pattern.

2). In the large lacunarity case, the holes are condensed at the centre of each square (cube) on each step of lattice construction; in the low lacunarity case, they are uniformly distributed throughout each square (cube).

Once the iterated procedure of lattice construction reaches a microscopic scale, we attach to each site i a spin σ_i which can be in any of q different Potts states. The Potts Hamiltonian (in units of $1/\beta = k_B T$) is

$$-\beta\mathcal{H} = \sum_{\langle i,j\rangle} J(q\delta_{\sigma_i\sigma_j} - 1) + \sum_{\langle i'j'\rangle} J_s(q\delta_{\sigma_{i'}\sigma_{j'}} - 1) \tag{2}$$

where $\langle ij\rangle$ and $\langle i'j'\rangle$ stand for first-neighbour pairs in the bulk or on inner surfaces bordering the holes, respectively.

The RG transformations are obtained using an approximate bond moving Migdal-Kadanoff scheme (Kadanoff 1976). It consists of moving all the bonds generated after n steps of lattice construction to the perimeter (or edge) of the squares (cubes) generated on the previous step (see figure 3). After decimating the remaining sites, the perimeter

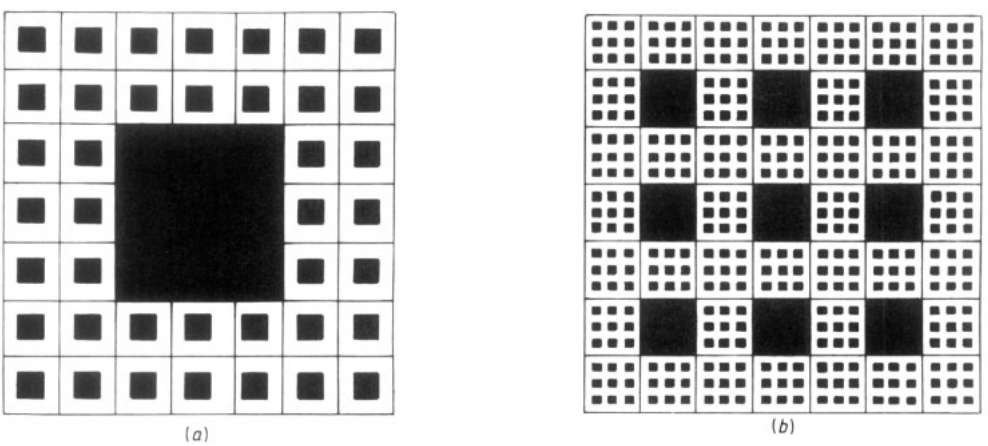

Figure 2. Sierpinski carpet with $b=7$, $l=3$ after two steps of lattice construction: (a) large lacunarity, (b) low lacunarity.

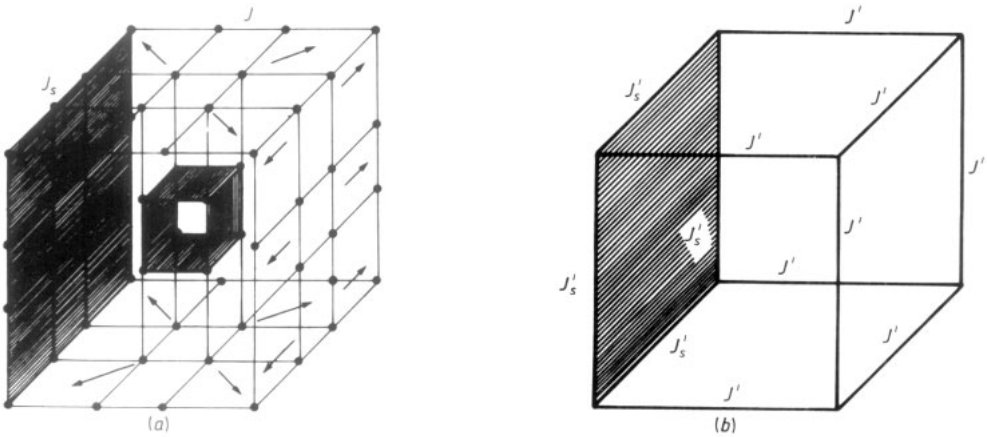

Figure 3. Illustration of a bond moving transformation on the Sierpinski pastry shell with $b=3$, $l=1$; (a) directions of bond moving applied to some vertical bonds; (b) renormalised interactions.

(edge) bonds are defined as J'_s or J', if they are bordering the holes of the lattice at the $(n-1)$ step or not.

The RG equations are expressed in the transmissivity variables t and t_s associated with antiferromagnetic bonds of strength J and J_s, respectively:

$$t=(1-\mathrm{e}^{-qJ})[1+(q-1)\,\mathrm{e}^{-qJ}]^{-1} \tag{3a}$$

$$t_s=(1-\mathrm{e}^{-qJ_s})[1+(q-1)\,\mathrm{e}^{-qJ_s}]^{-1}. \tag{3b}$$

One has, for the antiferromagnetic case, $-1/(q-1)\leqslant t,\ t_s\leqslant 0$, for temperatures $0\leqslant T\leqslant\infty$.

After the bond moving, the decimation procedure is carried out with the aid of the break-collapse method (Tsallis and Levy 1981), leading to the renormalised transmissivity variables (Riera and Chaves 1986)

$$t'=t_1^{b-l}\,t_2^{l} \tag{4a}$$

$$t'_s=t_3^{b-l}\,t_4^{l} \tag{4b}$$

with t_i $(i=1,4)$ given by

$$t_i^{\mathrm{D}}=(t^{\mathrm{D}})^{n_i}(t_s^{\mathrm{D}})^{s_i} \tag{5a}$$

where t^{D} stands for the dual variable:

$$t^{\mathrm{D}}=(1-t)[1+(q-1)t]^{-1}. \tag{5b}$$

The pair of values $(n_i,\ s_i)$ $(i=1,4)$ vary according to the lattices; for the carpet family with large lacunarity, we have

$$(n_1,\ s_1)=(b,0) \tag{6a}$$

$$(n_2,\ s_2)=(b-l-1,2) \tag{6b}$$

$$(n_3,\ s_3)=((b-1)/2,1) \tag{6c}$$

$$(n_4,\ s_4)=((b-l-2)/2,2) \tag{6d}$$

whereas for the low lacunarity family,

$$(n_1, s_1) = (b, 0) \tag{7a}$$

$$(n_2, s_2,) = (b-2l, 2l) \tag{7b}$$

$$(n_3, s_3) = ((b-1)/2, 1) \tag{7c}$$

$$(n_4, s_4) = ((b-1)/2-l, l+1). \tag{7d}$$

For the pastry family with large lacunarity, we have

$$(n_1, s_1) = (b^2, 0) \tag{8a}$$

$$(n_2, s_2) = (b^2-(l+1)^2, 4) \tag{8b}$$

$$(n_3, s_3) = (\tfrac{1}{4}(b-1)(3b+1), b) \tag{8c}$$

$$(n_4, s_4) = (n_3-\tfrac{3}{4}(l+1)^2, b+3) \tag{8d}$$

whereas for the low lacunarity family,

$$(n_1, s_1) = (b^2, 0) \tag{9a}$$

$$(n_2, s_2) = (b^2-4l^2, 4l^2) \tag{9b}$$

$$(n_3, s_3) = (\tfrac{1}{4}(b-1)(3b+1), b) \tag{9c}$$

$$(n_4, s_4) = (n_3-3l^2, b+3l^2). \tag{9d}$$

The RG equations obtained by this method allow us to consider non-integer values of q, so that we car assess how q_c varies with the geometrical parameters of the problem.

The phase diagrams in the t-t_s plane for the Sierpinski carpet family with central cutouts (b and l odd) are shown in figures 4 (for $q=2$) and 5 (for $q\neq 2$). The t-t_s coordinates for the fixed points of the RG equations (4) in the Ising case ($q=2$) are

$$\text{D: } (0,0) \qquad \text{O: } (-1,-1) \qquad \text{E: } (0,-1) \tag{10a}$$

$$\text{B: } (t^{\text{B}}, t_s^{\text{B}}) \qquad \text{A: } (t^{\text{A}}, -1) \qquad \text{C: } (-1,0). \tag{10b}$$

The trivial fixed points D and O are the sinks of the paramagnetic phase and the antiferromagnetic phase, respectively. The fixed point B governs the thermal transition of the bulk except for the $t_s=-1$ line ($J_s=-\infty$), which is governed by A. Fixed point E is associated with $T_c=0$ for the one-dimensional surfaces.

In figure 4 we show three distinct phase diagrams: (a) for $b=l+2$, $l\neq 1$; (b) for $l+4$, $l+6$, etc; (c) for $b=3$, $l=1$. When the 'surface' bonds are set equal to zero ($t_s=0$), lattices with $b=l+2$ become finitely ramified (Gefen *et al* 1984a), implying in $T_c=0$ (fixed point C in figures 4(a) and (c)). Also, for $J=-\infty$ ($t=-1$), systems with $b=l+4$, etc, are always ordered, irrespective of t_s (figure 4(b)); the same does not hold when $b=l+2$, $l\neq 1$ (figure 4(a)), although the case $b=3$, $l=1$ (figure 4(c)) can be regarded as marginal. These aspects illustrate the crucial role played by the 'surface' bonds to the onset of bulk order when $b=l+2$; to see this one should note that for b fixed, the connectivity is smaller when $l=b-2$ than when $l=b-4$, $b-6$, etc.

The phase diagrams and fixed points of the antiferromagnetic Ising model are symmetrically located in relation to the ones for the ferromagnetic case in the positive part of the t-t_s plane, obtained by the same bond moving scheme (Gefen *et al* 1984a). The location of fixed points A and B with their respective thermal exponents y_t are shown in table 1.

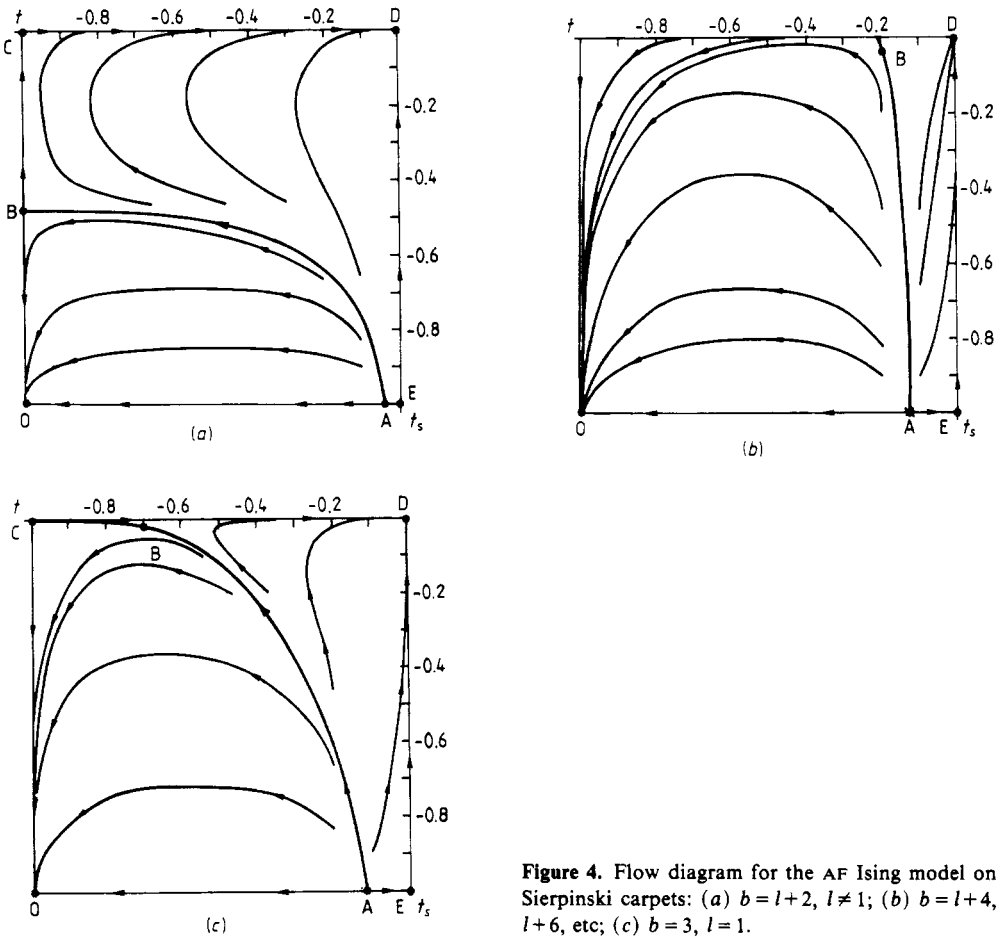

Figure 4. Flow diagram for the AF Ising model on Sierpinski carpets: (*a*) $b = l+2$, $l \neq 1$; (*b*) $b = l+4$, $l+6$, etc; (*c*) $b = 3$, $l = 1$.

For $q > 2$, the (t, t_s) coordinates of the fixed points of the RG equations (4) are (see figures 5(*a*) and (*b*))

$$\text{D: } (0, 0) \qquad \text{B: } (t^{\text{B}}, t_s^{\text{B}}) \qquad \text{O: } (t^{\text{O}}, t_s^{\text{O}}). \tag{11}$$

The new non-trivial fixed point O is the sink of the entire ordered phase, characterising this region by an infinite correlation length; in contrast to the $q = 2$ case, this phase is critical. As q increases from 2, the two fixed points B and O merge at a critical value q_c. For $q > q_c$, the system is always in the paramagnetic phase (figure 5(*c*)). The two regimes obtained when $q > 2$ can be understood from a ground state RG argument (Berker and Kadanoff 1980). If, among the ground state configurations, the probability that first-neighbour spins in the rescaled lattice are in the same state is of the same order as the probability of them being in different states, the $T = 0$ configuration characterises a disordered phase. By renormalisation, $T = 0$ flows to the ∞ temperature fixed point in the parameter space; if, on the other hand, the probability that first-neighbour spins in the rescaled lattice are in the same state is much smaller than the probability of them being in different states, the renormalisation flow will stop at some finite temperature fixed point in the parameter space. In the first case (for $q > q_c$) the number of states accessible to each spin in the AF ground state configurations has increased sufficiently to destroy any information about the state of a spin located a

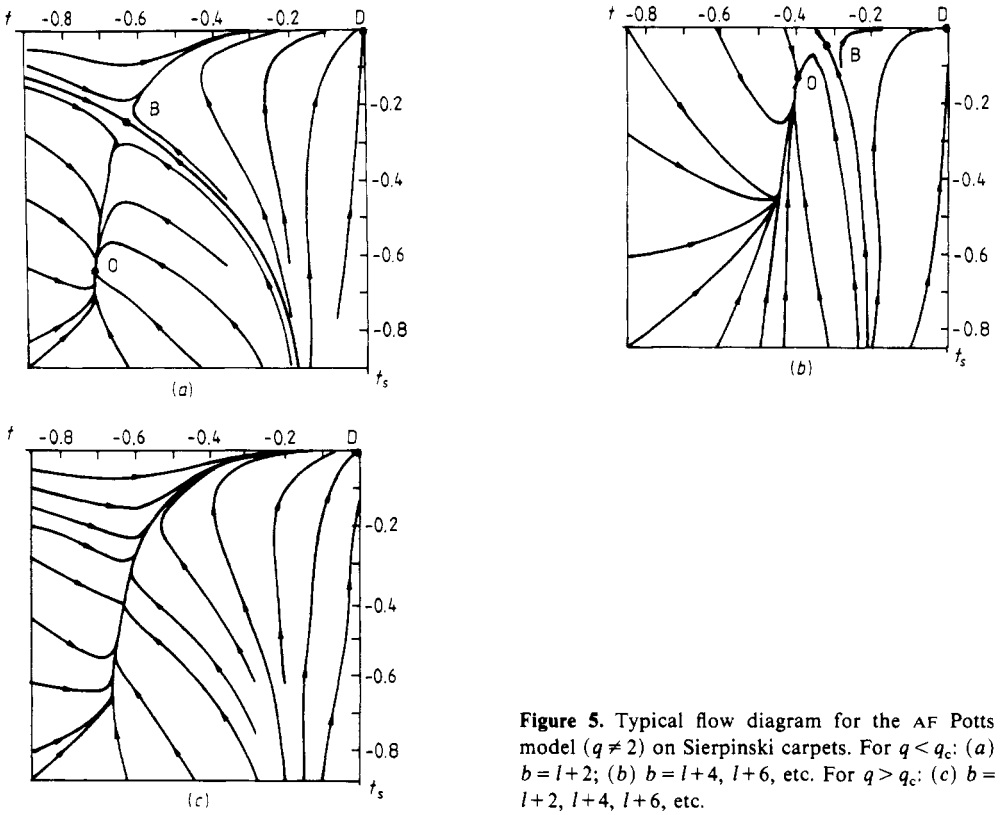

Figure 5. Typical flow diagram for the AF Potts model ($q \neq 2$) on Sierpinski carpets. For $q < q_c$: (a) $b = l+2$; (b) $b = l+4$, $l+6$, etc. For $q > q_c$: (c) $b = l+2$, $l+4$, $l+6$, etc.

'great' distance apart. In the second case ($q \leqslant q_c$) the opposite behaviour occurs: due to the geometrical constraints of the lattice, a change in the state of a spin at the origin must be followed by a change in the states of spins along a large region of the system if the ground state energy is to be kept fixed. Thus, the low temperature phase is characterised by an infinite correlation length, in constrast to AF systems with null ground state entropy per spin, such as the Ising model on a square lattice.

The phase diagrams for $2 < q \leqslant q_c$ are qualitatively different if $b = l+2$ (figure 5(a)) or if $b = l+4$, $l+6$, etc (figure 5(b)), although a critical phase is present in both cases. Also, as the system is one dimensional when $J = 0$ ($t = 0$), there is no phase transition at the t_s axis, even at $T = 0$, unlike the $q = 2$ case. When $J_s = -\infty$ ($t_s = -1/(q-1)$), the bulk is connected through the strong 'surface' bonds which implies a large T_c; the same occurs in the Ising case, but the critical behaviour at $t_s = -1/(q-1)$ near the critical line is governed by fixed point B. The differences between phase diagrams 5(a) and (b) are again due to the role of the 'surface' bonds in these geometries. In finite order of ramification when $J_s = 0$ ($t_s = 0$), for $b = l+2$ (figure 5(a)) implies that there is no transition on the t axis, whereas for $q = 2$ implies that $T_c = 0$. For these lattices one also sees that the surface bonds are crucial to the onset of bulk order and even when $J = -\infty$ ($t = -1/(q-1)$), the system has $T_c \neq 0$. The location of fixed points B and O and the thermal exponent y_T^B for some values of q are shown in table 1.

When the carpet family is constructed with the cutouts evenly distributed throughout the lattices (low lacunarity), the above picture does not change. There are two possible phase diagrams determined also by the roles of surface bonds to the onset of the

Table 1. Results for the antiferromagnetic Potts model on Sierpinski carpets.

b	l	D_f	q_c	q	t^B	t_s^B	y_T^B	t^A	y_T^A	t^O	t_s^O
(a) Large lacunarity											
3	1	1.893	2.14	2	−0.6992	−0.1568 E−1	0.2240	−0.1197	0.5620	—	—
				2.1	−0.6383	−0.2113	0.2602	—	—	−0.7447	−0.6764
5	1	1.975	2.18	2	−0.2048	−0.5378 E−2	0.6786	−0.1421	0.6707	—	—
				2.1	−0.2407	−0.1123 E−1	0.5086	—	—	−0.6190	−0.5654
5	3	1.722	2.05	2	−1.0	−0.4858	0.3836	−0.4108 E−1	0.4140	—	—
				2.1	—	—	—	—	—	—	—
7	1	1.989	2.17	2	−0.1501	−0.1783 E−1	0.6944	−0.1253	0.6829	—	—
				2.1	−0.1798	−0.4756 E−2	0.5187	—	—	−0.5119	−0.4586
7	3	1.896	2.10	2	−0.2682	−0.4531 E−2	0.5235	−0.8659 E−1	0.5942	—	—
				2.1	—	—	—	—	—	—	—
7	5	1.356	2.02	2	−1.0	−0.6629	0.3424	−0.2069 E−1	0.3492	—	—
				2.1	—	—	—	—	—	—	—
(b) Low lacunarity											
7	3	1.896	2.11	2	−1.0	−0.1448	0.4601	−0.0866	0.5942	—	—
				2.1	−0.4916	−0.2852	0.1836	—	—	−0.5104	−0.4322

ordered phase. Thus, for lattices with $b = 2l+1$, the AF order cannot propagate along 'interior' paths only and we are led to phase diagrams such as in figure 4(a) for $q = 2$ or as in figure 5(a) for $q \neq 2$ ($q \leqslant q_c$). Otherwise, for lattices with $b = 3l+2, 4l+3$, etc, we are led to figure 4(b) for $q = 2$ or to figure 5(b) for $q \neq 2$ ($q \leqslant q_c$).

Table 1 shows the values of q_c for several lattices of the carpet family. From this table, we see that for b fixed, q_c increases as D_f increases or for D_f fixed, q_c increases as the lacunarity L decreases. The effect of spreading out the holes is to relax the geometrical constraints to the onset of AF order (or to lower the mean coordination number of the lattice). This means that the order can flow along more independent paths which are achieved by considering the large number of paths bordering the holes. This mechanism is analogous to what occurs when the dimensionality of the system is increased, which leads to a larger value of q_c.

The fact that fractals with the same D_f but with different L yield different q_c suggests that AF systems exhibiting phase transitions on these two fractals should be on different universality classes.

The qualitative phase diagrams in the t-t_s plane for the pastry family for any $b \geqslant l+2$ (b and l odd) are shown in figure 6 for $q = 2$ and in figure 7 for $2 < q \leqslant q_c$. The fixed points of the RG equations for the Ising case are

$$\text{D: } (0, 0) \qquad \text{O: } (-1, -1) \qquad \text{E: } (0, -1) \tag{12a}$$

$$\text{B: } (t^B, t_s^B) \qquad \text{A: } (t^A, -1) \qquad \text{F: } (t^F, t_s^F) \qquad \text{G: } (0, t_s^G) \tag{12b}$$

where the location of the non-trivial ones are shown in table 2.

The trivial fixed points D, O and E are the sinks of the disordered phase (D), the bulk antiferromagnetic phase (BAF) and the surface antiferromagnetic phase (SAF) respectively. The non-trivial fixed points A and B govern the bulk critical behaviour while G governs the critical behaviour at the inner surfaces. The critical exponents across the FA, FB and FG critical lines (see figure 6) are governed by A, B and G

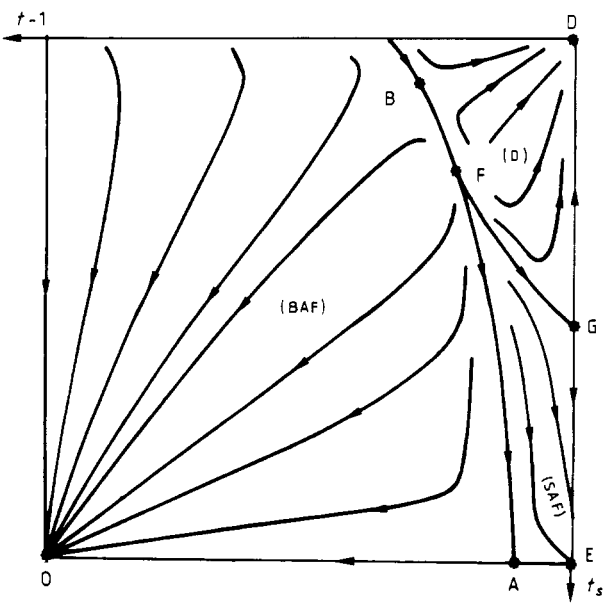

Figure 6. Flow diagram for the AF Ising model on Sierpinski pastry shells.

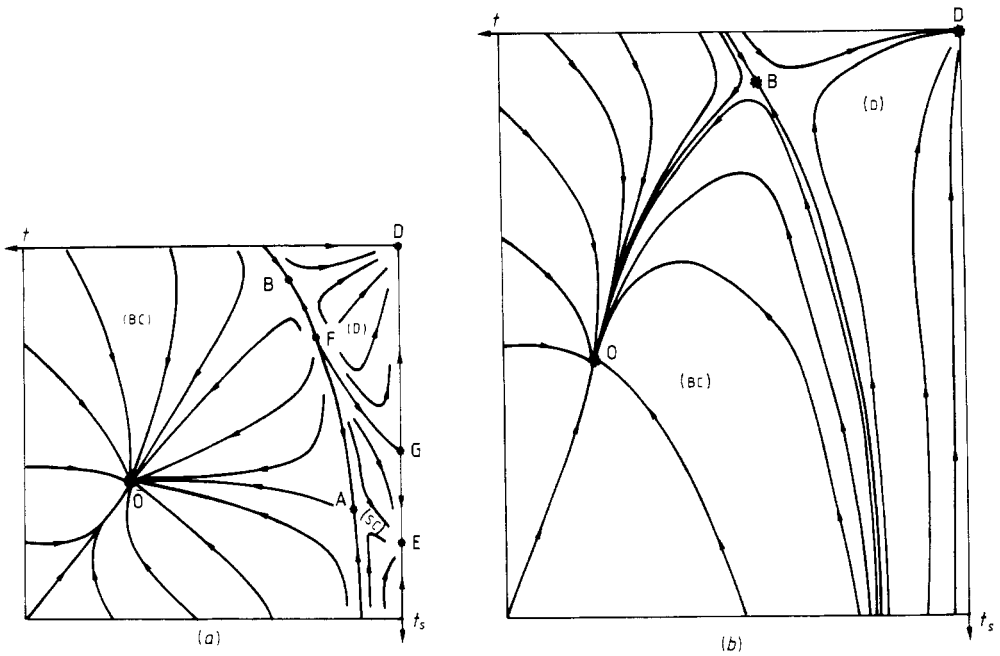

Figure 7. Typical flow diagram for the AF Potts model ($q \neq 2$) on Sierpinski pastry shells. (*a*) $q < q_c^s$, (*b*) $q_c^s < q < q_c$ (see text).

respectively. These lines join at the multicritical point F characterised by the parameter $\alpha_c = J_s^F/J^F$. Systems with $J_s/J > \alpha_c$ may exhibit an antiferromagnetic order at the inner surfaces without such order in the bulk. The values of α_c and of the thermal exponent y_T associated with A, G and B are shown in table 2.

Consider any fixed value of b and q and an increasing value of l in table 2. We find that the thermal exponent associated with the fixed point G goes in a direction opposite to the others. In fact, the G exponents must depend on parameters associated with the inner surfaces and here, while D_f decreases, the internal surface fractal dimensionality D_f^s increases. Also, from the values of t^A and t_s^G as l increases, we obtain increasing values of critical temperatures on the $t_s = -1$ and $t = 0$ lines respectively, showing the increasing contribution of the inner surfaces to the full geometry.

The fixed points of the RG equations for $2 < q \leq q_c$ are (see figure 7(*a*))

$$\text{D: } (0, 0) \qquad \text{O: } (t^O, t_s^O) \qquad \text{E: } (0, t_s^E) \tag{13a}$$

$$\text{B: } (t^B, t_s^B) \qquad \text{A: } (t^A, t_s^A) \qquad \text{F: } (t^F, t_s^F) \qquad \text{G: } (0, t_s^G). \tag{13b}$$

The fixed point D is the sink of the disordered phase (D) and O and E are the sink of critical phases in the bulk (BC) and at the inner surfaces (SC) respectively. The fixed point B governs the critical behaviour in the bulk between the BC-D phases and A governs the critical behaviour between the BC-SC phases. The fixed point G governs the critical behaviour between SC-D phases at the inner surfaces. The multicritical point F, as in the Ising case, characterises the crossover from the SC phase to the BC phase when $(J_s/J) = \alpha_c$.

As q increases from two, the fixed points E and G on the t_s axis merge when q reaches a value q_c^s. For $q > q_c^s$ the system does not exhibit any phase transition at the

Table 2. Results for the antiferromagnetic Potts model on Sierpinski pastry shells.

b	l	D_f	q_c^+	q_c	q	t_s^G	y_T^G	t_s^E	t^B	t_s^B	y_T^B	t^O	t_s^O	t^A	t_s^A	y_T^A	α_F
(a) Large lacunarity																	
3	1	2.9656	2.32	2.95	2.0	−0.1671	0.7511	—	−0.4851 E−1	−0.1318 E−1	0.9133	—	—	−0.1245 E−1	−1.0	0.6234	4.3
					2.3	−0.2618	0.2463	−0.3808	−0.5362 E−1	−0.1843 E−1	0.8141	−0.4551	−0.4551	−0.1739 E−1	−0.4075 E−1	0.5954	7.3
					2.9	—	—	—	−0.7957 E−1	−0.5633 E−1	0.3199	−0.1270	−0.1163	—	—	—	—
5	1	2.9950	2.23	2.74	2.0	−0.1552	0.7232	−1.0	−0.2044 E−1	−0.3433 E−2	0.9011	—	—	−0.1447 E−1	−1.0	0.8081	4.2
					2.2	−0.2266	0.3153	−0.3703	−0.2257 E−1	−0.4676 E−2	0.8270	−0.4019	−0.4019	−0.1882 E−1	−0.3881	0.7547	5.6
					2.3	—	—	—	−0.2395 E−1	−0.5630 E−2	0.7795	−0.2693	−0.2693	—	—	—	—
5	3	2.8488	2.27	2.55	2.0	−0.1196	0.7500	−1.0	−0.4648 E−1	−0.4182 E−2	0.7955	—	—	−0.1602 E−2	−1.0	0.4300	3.4
					2.2	−0.1600	0.4655	−0.3887	−0.5465 E−1	−0.8497 E−2	0.6674	−0.4019	−0.4019	−0.3151 E−2	−0.3903	0.4254	7.0
					2.3	—	—	—	−0.6000 E−1	−0.1403 E−1	0.5844	−0.2691	−0.2688	—	—	—	—
7	1	2.999	2.19	2.60	2.0	−0.1321	0.7102	−1.0	−0.1227 E−1	−0.1321 E−2	0.8841	—	—	−0.1032 E−1	−1.0	0.8360	5.0
					2.1	−0.1558	0.5558	−0.5122	−0.1301 E−1	−0.1634 E−2	0.8437	−0.5131	−0.5131	−0.1111 E−1	−0.5127	0.8016	5.7
					2.5	—	—	—	−0.1948 E−1	−0.6635 E−2	0.5082	−0.5803 E−1	−0.5663 E−1	—	—	—	—
7	3	2.9579	2.20	2.56	2.0	−0.1166	0.7179	−1.0	−0.1494 E−1	−0.1495 E−2	0.8686	—	—	−0.5775 E−2	−1.0	0.6853	4.9
					2.1	−0.1365	0.5764	−0.5125	−0.2234 E−1	−0.2582 E−1	0.7425	−0.5132	−0.5132	−0.6640 E−2	−0.5127	0.6668	5.9
					2.5	—	—	—	−0.2571 E−1	−0.1086 E−1	0.4046	−0.5677 E−1	−0.5382 E−1	—	—	—	—
(b) Low lacunarity																	
7	3	2.9579	2.21	2.57	2.0	−0.0872	0.6075	−1.0	−0.2452 E−1	−0.1932 E−2	0.7641	—	—	−0.5775 E−2	−1.0	0.6853	7.9
					2.1	−0.1090	0.4998	−0.5125	−0.2582 E−1	−0.2825 E−2	0.7366	0.5132	−0.5132	−0.6578 E−2	−0.5127	0.6660	8.7
					2.5	—	—	—	−0.2973 E−1	−0.1476 E−1	0.4266	−0.5800 E−1	−0.5654 E−1	—	—	—	—

inner surfaces (see figure 7(*b*)). For $q > q_c$ the system is always in the paramagnetic phase.

Table 2 shows the values q_c^s and q_c for the pastry family.

For a fixed b and increasing l, the values of q_c decreases (D_f decreases), but the value of q_c^s increases (D_f^s increases).

When the lacunarity is lowered, the effect on the values of q_c are the same as in the carpet family and the analysis follows along the same lines; the value of α_c also increases indicating that the fragmentation of the inner surfaces inhibits the onset of surface order without bulk order (by surface order we mean the simultaneous ordering of the surfaces bordering the holes, connected through the bulk).

To conclude, the behaviour of systems with non-zero ground state entropy per site are generally complex and the analysis of the order propagation in these systems leads to the possibility of an ordered phase characterised by an algebraic decay of correlations. For the q-state AF Potts model, this critical phase should occur for $q \leqslant q_c$, where the value of q_c is determined by the connectivity of the lattice. These arguments are general and can also be used in the context of fractal geometries.

Nevertheless, as the value of q_c for Euclidean lattices with dimension $d < 3$ is small, and the techniques used for dimensions $d \geqslant 3$ are incipient, the existence of such a critical phase is, as yet, still under investigation.

In this paper we generalise the results for the AF Potts model in the Migdal-Kadanoff approximation for fractal structures. Under this approximation, the results for the two families of fractals studied provide a qualitative description of the critical behaviour of the model from a geometric point of view.

One interesting result is that, besides depending on D_f, a fact observed for hypercubical lattices, q_c also depends on lacunarity. This new dependence of q_c comes from the fact that the fragmentation of vacant regions which occurs when the lacunarity decreases provides an increasing number of paths that include 'surface' bonds (in other words, increases the number of independent paths in the lattice). Thus, for the same D_f, as L is lowered, q_c must rise. This result suggests that AF Potts systems exhibiting phase transitions on fractals with the same D_f but different L should be in different universality classes. This is confirmed by the different values of thermal exponents obtained for these types of fractals. Besides, as illustrated in the $b = 7$, $l = 3$ case of the pastry family (table 2), as L decreases, the thermal exponents characterising the several transitions of the system also decrease. This behaviour is analogous to the effect of lowering D_f (or D_f^s) for lattices with the same value of b; both results were also obtained in the ferromagnetic case (Riera and Chaves 1986).

Since q_c increases as L decreases, one should expect that hypercubic lattices ($L = 0$) with non-integer dimension $d = D_f$ must have a larger q_c than a fractal lattice with the same D_f. This remark should be of interest in the context of ε expansions (Wilson and Kogut 1974). Also, from the behaviour of q_c with D_f and L, our results are in accord with the values $q_c\,(d = 2) = 2.3$ and $q_c\,(d = 3) = 3.3$ obtained for d-dimensional hypercubic lattices by Berker and Kadanoff (1980) using a similar bond moving scheme.

One should note that the bond moving approximation inhibits the propagation of the AF order along independent paths and thus the values of q_c obtained, including the ones of Berker and Kadanoff (1980), should be considered as a lower bound to the exact ones. Since this inhibition increases as b increases, we must only compare the results for lattices with the same value of b. Also, the effect of lowering q_c due to this approximation is stronger for low lacunarity, causing a reduction in the difference obtained between the values of q_c (and of q_c^s) in the low and large lacunarity cases.

Nevertheless, the different universality classes obtained for these lattices give support to the result that q_c (q_c^s) should be different for the two cases.

From the above analysis, and from the results for hypercubical lattices, namely the exact $T_c = 0$ for $q = 3$ on the square lattice (Baxter 1982) and the ordered low temperature phase for $q = 3$ and $q = 4$ on the simple cubic lattice (MC simulations, Banavar *et al* (1980)), we may conclude that the $q = 3$ AF Potts model must not show any phase transition on the Sierpinski carpets while it remains an open question if a critical phase indeed occurs for this model on the Sierpinski pastry shell.

Acknowledgments

I would like to thank Dr R R dos Santos for fruitful and friendly discussions and for critical readings of the manuscript and Dr C M Chaves for his kind encouragement.

References

Banavar J R, Grest G S and Jasnow D 1980 *Phys. Rev. Lett.* **45** 1424
Baxter R J 1982 *Proc. Phil. Soc.* A **43**
Berker A N and Kadanoff L P 1980 *J. Phys. A: Math. Gen.* **13** L259
Gefen Y, Aharony A and Mandelbrot B B 1984a *J. Phys. A: Math. Gen.* **17** 1277
Gefen Y, Aharony A, Shapir Y and Mandelbrot B B 1984b *J. Phys. A: Math. Gen.* **17** 435
Kadanoff L P 1976 *Ann. Phys., NY* **100** 359
Mandelbrot B B 1977 *Fractals: Form, Chance and Dimension* (San Francisco: Freeman)
Riera R 1985 *J. Phys. A: Math. Gen.* **18** L795
Riera R and Chaves C M 1986 *Z. Phys.* B **62** 387
Tsallis C and Levy S V F 1981 *Phys. Rev. Lett.* **47** 950
Wilson K G and Kogut K 1974 *Phys. Rep.* **12** 75